

Nucleosides

International Edition: DOI: 10.1002/anie.201910059
German Edition: DOI: 10.1002/ange.201910059

Enzymatic Incorporation of a Coumarin-Guanine Base Pair

Aaron Johnson, Ashkan Karimi, and Nathan W. Luedtke*

Abstract: Previous expansions beyond nature's preferred base-pairing interactions have utilized either nonpolar shape-fitting interactions or classical hydrogen bonding. Reported here is a hybrid of these systems. By replacing a single N–H with C–H at a Watson–Crick interface, the design space for new drug candidates and fluorescent nucleobase analogues is dramatically expanded, as demonstrated here by the new, highly fluorescent deoxycytidine mimic 3-glycosyl-5-fluoro-7-methoxy-coumarin-2'-deoxyribose (dC^C). $dGTP$ is selectively incorporated across from a template dC^C during enzymatic DNA synthesis. Likewise, dC^C is selectively incorporated across from a template guanine when dC^C is provided as the triphosphate dC^CTP . DNA polymerase I (Klenow fragment) exhibited about a 10-fold higher affinity for dC^CTP than $dCTP$, allowing selective incorporation of dC^C in direct competition experiments. These results demonstrate that a single C–H can replace N–H at a Watson–Crick-type interface with preservation of functional selectivity and enhanced activity.

Pairing beyond A–T and G–C gives fundamental insights into molecular recognition while providing tools for biotechnology and chemical biology.^[1] Benner et al. have produced an artificially expanded genetic information system (AEGIS) based on classical, multidentate hydrogen bonding.^[2] Tricyclic nucleobase pair scaffolds developed by Matsuda and co-workers expanded such logical designs to comprise four hydrogen bonds.^[3] In contrast, Romesberg et al. synthesized large libraries of nonpolar and non-isosteric base-pairing candidates and screened them for specific and orthogonal pairing behavior during DNA synthesis.^[4] Optimized “hits” from such screens have been applied in synthetic biology for creating bacteria with a six letter genetic alphabet,^[4c] aptamers,^[5] and expression platforms for producing RNAs and proteins containing non-natural residues.^[4d]

Base-pairing systems containing a combination of classical and nonclassical hydrogen-bonding interactions have not been previously reported. If successful, this approach would loosen the design restrictions for producing new, functional nucleosides as drug candidates,^[6] as well as highly fluorescent nucleobase analogues.^[7] The potential for a CH group to act as a nonclassical hydrogen-bond donor in a Watson–Crick interface was previously evaluated in the context of the nonpolar thymidine isostere difluorotolyl deoxyribose **F**.^[8] Kool et al. demonstrated that **F** could be selectively incorpo-

rated across from deoxyadenosine (**dA**) and vice versa in primer extension reactions.^[9] A subsequent X-ray structure revealed a nearly coplanar orientation of the **F**–**dA** base pair in duplex DNA,^[8d] yet, according to thermal denaturation experiments, **F**–**dA** base pairs provided little or no thermal stabilization of duplex DNA.^[8b] Computational studies concluded that **F**–**dA** pairing in the active site of DNA polymerase was due to shape complementary between **F** and **dA**, and that any hydrogen-bonding interactions were very weak due to the low polarity of **F**.^[9g]

Here we report the trisubstituted coumarin dC^C (Figure 1 a), which mimics deoxycytidine (**dC**) during enzymatic synthesis of DNA. A multidentate interface containing

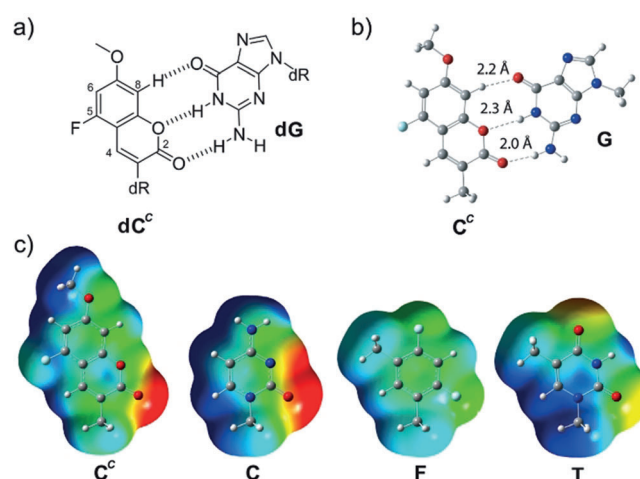


Figure 1. a) Proposed dC^C – dG base pair and coumarin numbering. b) Optimized structure of C^C –**G** in the gas phase according to B3LYP/6–31 + G(d).^[10] c) Electrostatic potential maps on van der Waals surfaces of C^C , **C**, **F**, and **T** bases containing methyl groups rather than deoxyribose (**dR**). Scale: –50 to +25 kcal mol^{–1}; calculated using B3LYP/6–31 + G(d) in water. See Table S1 for dipole moments and partial atomic charges.

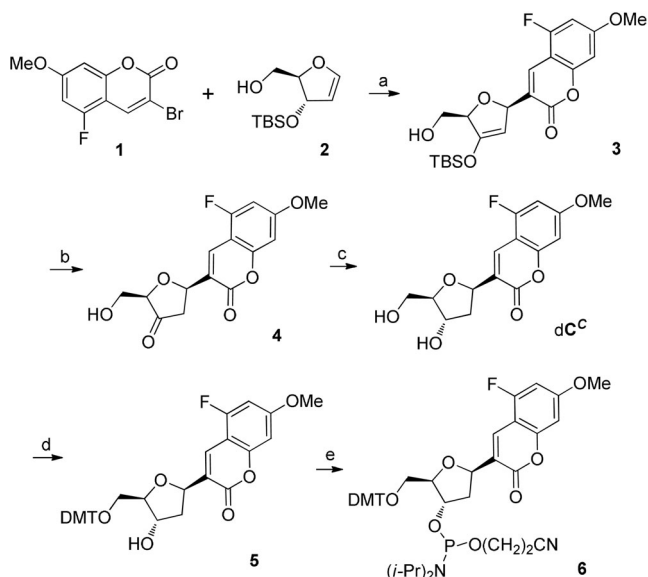
classical and nonclassical hydrogen bonds in dC^C – dG pairs is supported by density-functional theory (DFT) calculations (Figure 1 b), as well as structure–activity relationships in the enzymatic incorporation and elongation efficiencies of 10 different purine dNTPs across from dC^C . Only $dGTP$ itself and highly related analogues (7-deaza- $dGTP$, 6-thio- $dGTP$ and $dITP$) were efficient substrates for incorporation, whereas all dNTPs lacking a hydrogen bond acceptor at C6 were rejected as substrates. Together these results support the presence of a functional, multidentate pairing interaction between dC^C and dG in the active site of a high-fidelity DNA polymerase.

[*] Dr. A. Johnson, A. Karimi, Prof. Dr. N. W. Luedtke
Department of Chemistry, University of Zurich
Winterthurerstrasse 190, 8057 Zurich (Switzerland)
E-mail: nathan.luedtke@chem.uzh.ch

Supporting information and the ORCID identification number(s) for the author(s) of this article can be found under:
<https://doi.org/10.1002/anie.201910059>.

The design of dC^C was based on previous studies showing that substituents at the 4- and 5-positions of pyrimidines are well accommodated in the major groove of duplex DNA and are compatible with the enzymatic synthesis of DNA and RNA.^[11] The 3-position of coumarin was used as the attachment point to deoxyribose to provide a Watson–Crick face mimic of cytosine.^[12] DFT calculations confirmed that proper hydrogen-bonding geometries and distances could be achieved by multidentate pairing of dC^C – dG (Figure 1b). To increase the polarity of the coumarin scaffold while endowing favorable fluorescence properties,^[13] methoxy was placed at the 7-position and fluorine at the 5-position. This design was evaluated using DFT calculations (Figure 1c; see Table S1 in the Supporting Information). Addition of the 7-methoxy group increased the dipole moment of the coumarin scaffold by 1.8 Debye, giving a value similar to that of cytosine itself (see Table S1). The base stacking propensity of the heterocycle,^[8c] as well as the partial atomic charge (NBO) of C–H at the 8-position (see Table S1) were enhanced by including a fluorine at the 5-position. The final electrostatic potential map of dC^C revealed a similar pattern along the Watson–Crick face as compared to dC (Figure 1c), and furthermore highlighted the large differences in polarity between dC^C and **F**.

The bromo-fluoro-methoxycoumarin **1** was synthesized according to the steps in Scheme S1. Cross-coupling of **1** with the glycol **2** by a Heck reaction proceeded in a diastereoselective fashion (Scheme 1).^[14] The resulting silyl enol ether **3** was deprotected to afford the ketone **4**. Finally, diastereoselective reduction and purification delivered the new C-



Scheme 1. Synthesis of the dC^C nucleoside and phosphoramidite. Reagents and conditions: a) palladium(II) acetate, tri(*o*-tolyl)phosphine, triethylamine, THF, 66 °C, 16 h; b) hydrogen fluoride pyridine, THF, 0 °C to 26 °C, 1 h; c) sodium triacetoxyborohydride, acetic acid, acetonitrile, 0 °C to 27 °C, 2.5 h, 10% over 3 steps; d) 4,4'-dimethoxytrityl chloride, pyridine, 26 °C, 20 h, 33%; e) 2-cyanoethyl *N,N*-diisopropylchlorophosphoramidite, *N,N*-diisopropylethylamine, DCM, 0 °C to 26 °C, 1 h, 89%. DCM = dichloromethane, DMT = 4,4'-dimethoxytrityl, TBS = *tert*-butyldimethylsilyl, THF = tetrahydrofuran.

nucleoside dC^C as a single diastereomer in 10% yield over the three steps. A β configuration of the anomeric center was confirmed by NOESY NMR spectroscopy. Consistent with other reports of 7-substituted coumarins,^[13,15] dC^C is an intensively bright fluorophore with a quantum yield of $\Phi = 0.71$ and molar extinction coefficient $\epsilon = 15,200 \text{ cm}^{-1}\text{M}^{-1}$ in water (see Figure S1). The product of these terms ($10800 \text{ cm}^{-1}\text{M}^{-1}$) makes dC^C one of the brightest fluorescent nucleobase analogues reported to date.^[17] Consistent with the presence of base-stacking interactions and excited-state electron transfer, quenching of dC^C was observed in both single-stranded (brightness = $79\text{--}1300 \text{ cm}^{-1}\text{M}^{-1}$) and double-stranded DNA (brightness = $59\text{--}301 \text{ cm}^{-1}\text{M}^{-1}$; see Table S2).

To evaluate the coding selectivity of dC^C when located in a template strand, the dC^C phosphoramidite **6** (Scheme 1) was synthesized and incorporated into oligonucleotides using automated DNA synthesis. The dC^C -containing oligonucleotides were purified using HPLC and annealed to complementary primers to give a primer–template duplex containing an 11 nucleotide 5'-overhang (Figure 2). Primer extension



Figure 2. a) PEX reactions containing dGTP, dATP, dCTP, and dTTP at various time points (min.). b) Reactions containing only dATP, dCTP, and dTTP. All reactions contained 100 nM template + primer, $2 \mu\text{M}$ of each dNTP, and 50 nM DNA polymerase (Klenow fragment). Aliquots were removed at various time points and quenched with 10 M urea and resolved using 20% DPAGE. FAM = fluorescein, M = molecular weight markers. For comparison with deoxycytidine see Figure S3.

(PEX) reactions were conducted in the presence of dGTP, dATP, dCTP, and dTTP (Figure 2a). Alternatively, a mixture of dATP, dCTP, and dTTP, lacking dGTP was used (Figure 2b). Full-length products [see Figures S2 and S3; MALDI-TOF-MS (calc. for $C_{282}H_{349}N_{91}O_{170}P_{26} = 8534$; observed 8539)] were only observed in reactions containing all four dNTPs, whereas stalling of primer extension across from dC^C was observed in reactions lacking dGTP (Figure 2b).

To evaluate the thermal stabilities (T_m) of duplexes containing dC^C , synthetic oligonucleotides containing dC^C were annealed to complementary sequences containing a variable residue (dA, dT, dG, dC, or an abasic site) across from dC^C (see Table S3). While duplexes containing dC^C were less thermally stable ($-\Delta T_m = 2.5\text{--}6.2 \text{ }^\circ\text{C}$) than duplexes containing only canonical base pairs, they were more stable than duplexes containing an abasic site ($-\Delta T_m = 6.4\text{--}8.0 \text{ }^\circ\text{C}$). When a purine residue was located across from dC^C , losses in thermal stability ($-\Delta T_m$) were in the range of 2.5–3.5 °C. Larger losses in thermal stability ($-\Delta T_m = 4.2\text{--}6.2 \text{ }^\circ\text{C}$) were observed when a pyrimidine residue was in the opposite

strand. These results are consistent with dC^C behaving like a pyrimidine residue in terms of its impact on T_m values, since pyrimidine–pyrimidine mismatches are among the most destabilizing mismatches in duplex DNA.^[16] According to our T_m data, dC^C was unable to discriminate between dA and dG in the opposite strand. However, the variable contributions made by enthalpy and entropy can result in T_m values that do not necessarily reflect energetic trends at lower temperatures.^[17]

To characterize the base-pairing selectivity of dC^C under physiological conditions with respect to temperature (37 °C) and salt, we conducted primer extension reactions using DNA polymerase I (Klenow fragment) and 10 different, non-canonical nucleotide triphosphates (Figure 3). Among these,

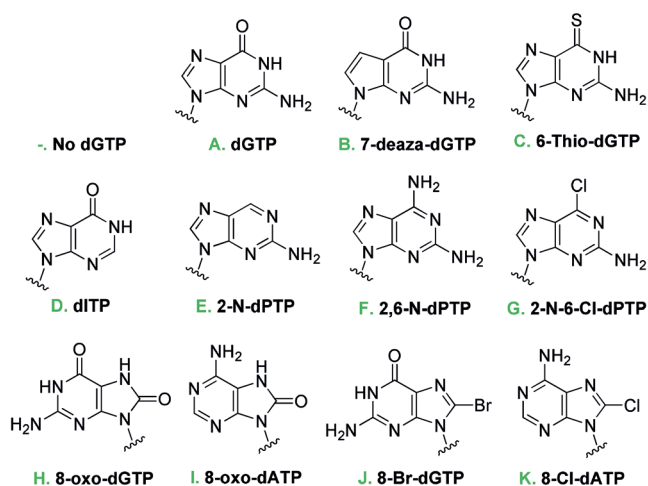


Figure 3. Nucleobase structures of dNTPs used in PEX reactions.

7-deaza-dGTP and 6-thio-dGTP (B, C) were chosen because of their high structural similarity with dGTP. Triphosphates with perturbed Watson–Crick faces were also examined, including dITP (D), which is considered to be a “universal” base.^[18] 2-Aminopurine (E) usually pairs with thymine but can occasionally pair with cytosine.^[19] 2,6-Diaminopurine (F) exhibits selectivity for thymine but also causes “knock on” effects in duplex DNA.^[20] Finally, 8-substituted derivatives containing a *syn* glycosidic bond were assessed (H–K). Primer extension reactions were conducted with one dNTP (A–K) in the presence of dATP, dCTP, and dTTP. Only dGTP itself and highly related analogues (7-deaza-dGTP, 6-thio-dGTP and dITP) were efficient substrates, giving full-length products (Figure 4). Notably, all four of these dNTPs contain a (thio)-carbonyl group at the 6-position, an NH at the 1-position, and an *anti* glycosidic bond. Together these results suggest a highly specific, multidentate interaction in dC^C –dG base pairing under physiological conditions, consistent with a nonclassical, C–H...O=C hydrogen bond in the active site of the polymerase.

The base-pairing selectivity of dC^C was further evaluated using dC^C triphosphate (dC^C TP, for synthesis see Scheme S2). PEX reactions using four different templates containing a single nucleotide 5'-overhang “X” = dA, dT, dG, or dC

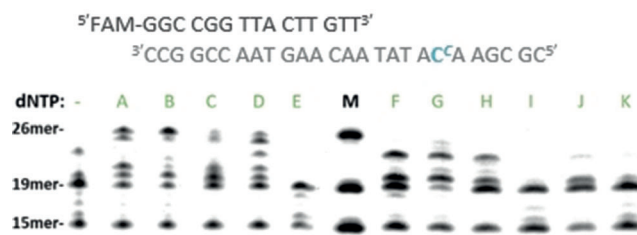


Figure 4. PEX reactions with variable dNTPs annotated in Figure 3 and conducted as in Figure 2 after only 5 minute reaction times. See Figure S5 for additional replicates.



Figure 5. PEX reactions of four different duplexes in the presence of dC^C TP. Each reaction contained 20 nM template + primer, 2 nM of DNA polymerase (Klenow fragment) and 400 nM of dC^C TP. Aliquots were quenched with 10 M urea and analyzed using 18% DPAG at 60 °C.

(Figure 5). Primer elongation was most efficient for X = dG. The product contained dC^C according to MALDI-TOF-MS (calc. for $C_{189}H_{225}F_1N_{52}O_{110}P_{16}$ = 5,497; observed 5,499). Initial velocities (V_0) measured under conditions of saturating dC^C TP and saturating DNA template were 3- to 15-fold higher for X = dG ($V_0 = 1.5 \pm 0.2$ nm min⁻¹ per nM enzyme) as compared to X = dA, dT or dC ($V_0 = 0.1$ – 0.5 nm min⁻¹ per nM enzyme; see Figure S5a). In the case of X = dG, the apparent K_m for dC^C TP was unexpectedly in the range of 40–400 nM (see Figure S5b), reflecting an approximate 10-fold higher affinity of the enzyme for dC^C TP than dCTP itself (see Figure S5c). Indeed, in direct competition PEX reactions containing a 1:1 ratio of both dC^C TP and dCTP, only dC^C could be detected in the product (see Figure S6). The resulting dC^C nucleotide at the 5'-end of the primer was competent for further elongation, according to PEX reactions conducted using a template with a five-nucleotide 5'-overhang (X = GTTTT³). The primer was extended to the expected full-length product in the presence of both dC^C TP and dATP (Figure 6a), whereas misincorporation of dA into the primer in the absence of dC^C TP resulted in chain termination (Figure 6b).

In summary, dC^C is the first example of a nucleobase analogue containing both polar and nonpolar hydrogen bonding in a multidentate array. DNA polymerase I (Klenow fragment) exhibited about a 10-fold higher affinity for dC^C TP than dCTP, allowing the selective incorporation of dC^C across from dG in direct competition experiments with dCTP. These results demonstrated that a single C–H can replace N–H in a Watson–Crick-type interface with partial preservation of functional specificity and even some enhanced activities. In some ways, dC^C was less functional than native dC (ex. kcat, processivity, base pairing fidelity), and in some ways, dC^C was more functional than native dC (ex. polymerase affinity, fluorescence properties). The altered functionality of dC^C suggests possible applications of this

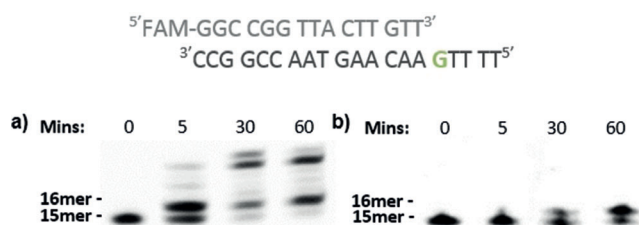


Figure 6. Primer extension reactions in the presence of a) both dC^CTP and dATP and b) dATP alone. Each reaction contained 50 nM of template + primer, 2 μM of dC^CTP and/or dATP, and 50 nM of polymerase.

approach in the development of new anticancer and antiviral agents.^[6]

dC^C-dG base pairing interactions exhibited the combined properties of standard Watson-Crick base pairing and non-polar interactions that are present, for example, in difluorotolyl deoxyribose (F)-dA. This pair is known to be coplanar in duplex DNA, selective in primer extension reactions, and yet it lacks the same stability and specificity of Watson-Crick base pairs during thermal denaturation of duplex DNA.^[8,9] Unlike F, however, dC^C was able to discriminate between purines and pyrimidines in the opposite strand according to T_m measurements.

In addition to demonstrating a new type of base pairing mimicry and design strategy, dC^C provides one of the brightest fluorescent nucleobase mimics reported to date.^[7] This new approach of utilizing a C-nucleoside capable of both classical and nonclassical hydrogen bonding should be applicable to the incorporation of fluorophores, with greatly improved brightness, into DNA and RNA.

Acknowledgements

We gratefully acknowledge the Swiss National Science Foundation for generous financial support (grant 165949).

Conflict of interest

The authors declare no conflict of interest.

Keywords: DNA · fluorescent probe · hydrogen bonding · noncovalent interactions · nucleosides

- [1] a) A. T. Krueger, H. Lu, A. H. F. Lee, E. T. Kool, *Acc. Chem. Res.* **2007**, *40*, 141–150; b) J. Štambaský, M. Hocek, P. Kočovský, *Chem. Rev.* **2009**, *109*, 6729–6764; c) D. A. Malyshev, F. E. Romesberg, *Angew. Chem. Int. Ed.* **2015**, *54*, 11930–11944; *Angew. Chem.* **2015**, *127*, 12098–12113; d) E. Biondi, S. A. Benner, *Biomedicines* **2018**, *6*, 53.
- [2] a) S. A. Benner, *ACS Cent. Sci.* **2016**, *2*, 882–884; b) S. Hoshika, I. Singh, C. Switzer, R. W. Molt, N. A. Leal, M.-J. Kim, M.-S. Kim, H.-J. Kim, M. M. Georgiadis, S. A. Benner, *J. Am. Chem.*

Soc. **2018**, *140*, 11655–11660; c) S. Hoshika, N. A. Leal, M.-J. Kim, M.-S. Kim, N. B. Karalkar, H.-J. Kim, A. M. Bates, N. E. Watkins, H. A. SantaLucia, A. J. Meyer, S. DasGupta, J. A. Piccirilli, A. D. Ellington, J. SantaLucia, M. M. Georgiadis, S. A. Benner, *Science* **2019**, *363*, 884–887.

- [3] a) N. Minakawa, N. Kojima, S. Hikishima, T. Sasaki, A. Kiyosue, N. Atsumi, Y. Ueno, A. Matsuda, *J. Am. Chem. Soc.* **2003**, *125*, 9970–9982; b) S. Hikishima, N. Minakawa, K. Kuramoto, S. Ogata, A. Matsuda, *ChemBioChem* **2006**, *7*, 1970–1975; c) N. Minakawa, S. Ogata, M. Takahashi, A. Matsuda, *J. Am. Chem. Soc.* **2009**, *131*, 1644–1645.
- [4] a) M. Berger, A. K. Ogawa, D. L. McMinn, Y. Wu, P. G. Schultz, F. E. Romesberg, *Angew. Chem. Int. Ed.* **2000**, *39*, 2940–2942; *Angew. Chem.* **2000**, *112*, 3069–3071; b) M. Berger, S. D. Luzzi, A. A. Henry, F. E. Romesberg, *J. Am. Chem. Soc.* **2002**, *124*, 1222–1226; c) D. A. Malyshev, K. Dhami, T. Lavergne, T. Chen, N. Dai, J. M. Foster, I. R. Corrêa, F. E. Romesberg, *Nature* **2014**, *509*, 385; d) Y. Zhang, J. L. Ptacin, E. C. Fischer, H. R. Aerni, C. E. Caffaro, K. San Jose, A. W. Feldman, C. R. Turner, F. E. Romesberg, *Nature* **2017**, *551*, 644.
- [5] K. Hamashima, Y. T. Soong, K.-i. Matsunaga, M. Kimoto, I. Hirao, *ACS Synth. Biol.* **2019**, *8*, 1401–1410.
- [6] K. L. Seley-Radtke, M. K. Yates, *Antiviral Res.* **2018**, *154*, 66–86.
- [7] a) W. Xu, K. M. Chan, E. T. Kool, *Nat. Chem.* **2017**, *9*, 1043–1055; b) A. R. Rovira, A. Fin, Y. Tor, *Chem. Sci.* **2017**, *8*, 2983–2993; c) M. Bood, A. F. Führtbauer, M. S. Wranne, J. J. Ro, S. Sarangamath, A. H. El-Sagheer, D. L. M. Rupert, R. S. Fisher, S. W. Magennis, A. C. Jones, F. Höök, T. Brown, B. H. Kim, A. Dahlén, L. M. Wilhelmsson, M. Grøtli, *Chem. Sci.* **2018**, *9*, 3494–3502.
- [8] a) B. A. Schweitzer, E. T. Kool, *J. Org. Chem.* **1994**, *59*, 7238–7242; b) B. A. Schweitzer, E. T. Kool, *J. Am. Chem. Soc.* **1995**, *117*, 1863–1872; c) J. S. Lai, J. Qu, E. T. Kool, *Angew. Chem. Int. Ed.* **2003**, *42*, 5973–5977; *Angew. Chem.* **2003**, *115*, 6155–6159; d) S. Pradeep, M. Egli, *J. Am. Chem. Soc.* **2009**, *131*, 12548–12549.
- [9] a) D. Liu, S. Moran, E. T. Kool, *Chem. Biol.* **1997**, *4*, 919–926; b) S. Moran, R. X.-F. Ren, E. T. Kool, *J. Am. Chem. Soc.* **1997**, *119*, 2056–2057; c) S. Moran, R. X.-F. Ren, E. T. Kool, *Proc. Natl. Acad. Sci. USA* **1997**, *94*, 10506–10511; d) E. T. Kool, *Annu. Rev. Biophys. Biomol. Struct.* **2001**, *30*, 1–22; e) E. T. Kool, *Annu. Rev. Biochem.* **2002**, *71*, 191–219; f) E. T. Kool, H. O. Sintim, *Chem. Commun.* **2006**, 3665–3675; g) O. Khakhshoor, S. E. Wheeler, K. N. Houk, E. T. Kool, *J. Am. Chem. Soc.* **2012**, *134*, 3154–3163.
- [10] Y. Zhao, N. E. Schultz, D. G. Truhlar, *J. Chem. Phys.* **2005**, *123*, 161103.
- [11] a) L. M. Wilhelmsson, P. Sandin, A. Holmén, B. Albinsson, P. Lincoln, B. Nordén, *J. Phys. Chem. B* **2003**, *107*, 9094–9101; b) S. Jäger, G. Rasched, H. Kornreich-Leshem, M. Engeser, O. Thum, M. Famulok, *J. Am. Chem. Soc.* **2005**, *127*, 15071–15082; c) G. Stengel, B. W. Purse, L. M. Wilhelmsson, M. Urban, R. D. Kuchta, *Biochemistry* **2009**, *48*, 7547–7555; d) A. Hottin, A. Marx, *Acc. Chem. Res.* **2016**, *49*, 418–427; e) H. Cahová, A. Panattoni, P. Kielkowski, J. Fanfrlík, M. Hocek, *ACS Chem. Biol.* **2016**, *11*, 3165–3171; f) H. M. Kropp, S. L. Dürr, C. Peter, K. Diederichs, A. Marx, *Proc. Natl. Acad. Sci. USA* **2018**, *115*, 9992–9997.
- [12] Coumarin analogs have been previously incorporated into DNA but never as nucleobase mimics: a) E. B. Brauns, M. L. Madaras, R. S. Coleman, C. J. Murphy, M. A. Berg, *J. Am. Chem. Soc.* **1999**, *121*, 11644–11649; b) D. Andreatta, J. L. Pérez Lustres, S. A. Kovalenko, N. P. Ernsting, C. J. Murphy, R. S. Coleman, M. A. Berg, *J. Am. Chem. Soc.* **2005**, *127*, 7270–7271; c) R. S. Coleman, M. A. Berg, C. J. Murphy, *Tetrahedron* **2007**, *63*, 3450–3456; d) H. Sun, H. Fan, X. Peng, *J. Org. Chem.* **2014**, *79*, 11359–11369; e) H. M. Mojibul, S. Huabing, L. Shuo, W. Yinsheng, P.

- Xiaohua, *Angew. Chem. Int. Ed.* **2014**, *53*, 7001–7005; *Angew. Chem.* **2014**, *126*, 7121–7125.
- [13] a) J. S. Seixas de Melo, R. S. Becker, A. L. Macanita, *J. Phys. Chem.* **1994**, *98*, 6054–6058; b) A. Takadate, T. Masuda, C. Murata, T. Tanaka, M. Irikura, S. Goya, *Anal. Sci.* **1995**, *11*, 97–101; c) W.-C. Sun, K. R. Gee, R. P. Haugland, *Bioorg. Med. Chem. Lett.* **1998**, *8*, 3107–3110.
- [14] M. Minuth, C. Richert, *Angew. Chem. Int. Ed.* **2013**, *52*, 10874–10877; *Angew. Chem.* **2013**, *125*, 11074–11077.
- [15] a) W. R. Sherman, E. Robins, *Anal. Chem.* **1968**, *40*, 803–805; b) L. Cong, H. Yin, Y. Shi, M. Jin, D. Ding, *RSC Adv.* **2015**, *5*, 1205–1212; c) X. Liu, Q. Qiao, W. Tian, W. Liu, J. Chen, M. J. Lang, Z. Xu, *J. Am. Chem. Soc.* **2016**, *138*, 6960–6963; d) G. Bassolino, C. Nancoz, Z. Thiel, E. Bois, E. Vauthey, P. Rivera-Fuentes, *Chem. Sci.* **2018**, *9*, 387–391.
- [16] a) F. Aboul-ela, D. Koh, I. Tinoco, F. H. Martin, *Nucleic Acids Res.* **1985**, *13*, 4811–4824; b) B. L. Gaffney, R. A. Jones, *Biochemistry* **1989**, *28*, 5881–5889.
- [17] A. S. Benz, G. Mata, O. P. Schmidt, N. W. Luedtke, *Nucleic Acids Res.* **2018**, *46*, 6470–6479.
- [18] F. H. C. Crick, *J. Mol. Biol.* **1966**, *19*, 548–555.
- [19] D. H. Persing, L. McGinty, C. W. Adams, *Mutat. Res. Fundam. Mol. Mech. Mutagen.* **1981**, *83*, 25–37.
- [20] C. Bailly, M. J. Waring, *Nucleic Acids Res.* **1998**, *26*, 4309–4314.

Manuscript received: August 7, 2019

Accepted manuscript online: September 4, 2019

Version of record online: ■ ■ ■ ■ ■, ■ ■ ■ ■ ■

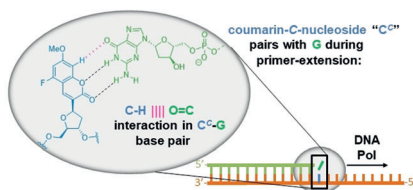
Communications



Nucleosides

A. Johnson, A. Karimi,
N. W. Luedtke* ————— ■■■■-■■■■

Enzymatic Incorporation of a Coumarin-
Guanine Base Pair



Replacements: A single C–H can replace N–H at a Watson–Crick-type interface with preservation of functional selectivity and enhanced activity. As demonstrated here, dGTP is selectively incorporated across from the new, highly fluorescent deoxycytidine mimic 3-glycosyl-5-fluoro-7-methoxy-coumarin-2'-deoxyribose (dC^C) during enzymatic DNA synthesis. Likewise, dC^CTP is selectively incorporated across from a guanine template.